# Original Paper

## Method for determination of in-vitro fiber dissolution rate by direct optical measurement of diameter decrease

Russell M. Potter

Owens Corning Science and Technology Center, Granville, OH (USA)

A new method for measuring in-vitro fiber dissolution rate in physiological saline solutions is based on direct optical measurement of fiber diameter decrease. Dissolution times measured by this new method for a variety of vitreous silicate fibers with a wide range of dissolution rates are in good agreement with results from SEM and from traditional mass loss and solution analysis techniques. The new method is conceptually and experimentally simple, and it can be applied directly to fibers pulled from the original fiber sample with no pretreatment.

**Methode zur Bestimmung der In-vitro-Auflösungsrate von Glasfasern durch direkte optische Messung der Durchmesserabnahme**

Es wird eine neue Methode zur Messung der In-vitro-Auflösungsrate von Glasfasern in physiologischen Kochsalzlösungen vorgestellt, die die Abnahme des Faserdurchmessers optisch direkt mißt. Die mit dieser Methode für eine Anzahl von Glasfasern mit sehr unterschiedlichen Auflösungsraten gemessenen Auflösungszeiten stimmen gut mit Ergebnissen überein, die mit dem SEM-Verfahren sowie mit traditionellen Gewichtsverlust- und Lösungstechniken erreicht wurden. Konzeption und experimentelle Durchführung der neuen Methode sind einfach. Sie kann direkt auf Fasern angewandt werden, die ohne Vorbehandlung von der Originalfaserprobe gezogen werden.

### 1. Introduction

For about the last 20 years there has been interest in the dissolution rate of fibers in model physiological fluids thought to simulate the environment in the lung. This interest has intensified in recent years as the link between a fiber's durability and its association with lung disease has been clearly identified [1 to 4]. Throughout this time a number of different in-vitro laboratory techniques have been developed and used to quantify fiber dissolution [for example, 5 to 21]. These differ in the pH and chemical composition of the model physiological fluid, in the flow rate of fluid past the fibers, in the nature of the measurements used to assess the fiber dissolution rate, and in the way in which the dissolution rate is calculated and expressed. There is general consensus that flow-through techniques which minimize alteration of the fluid by the dissolving fibers model most accurately the environment in-vivo [19]. The most widely used analytical method has been chemical analysis of the fluid for one or more of the dissolving components. The mass loss is calculated from these data, and a dissolution rate constant is derived from the mass loss. The dissolution rate is most commonly expressed as $k_{dis}$, the mass loss in units of ng/(cm$^2$ h). It is also expressed as a dissolution velocity in various units of length per time.

Received 27 September, revised manuscript 23 November 1999.

Despite the success of the various in-vitro methods in measuring fiber durability, there are a number of fundamental and practical problems with the available methods that have prevented a general acceptance of any one as a universal standard. Besides the overriding requirement of good correlation with in-vivo data, such a standard in-vitro fiber dissolution rate measurement technique would have the following attributes:

a) Conceptual simplicity: Biopersistence of long fibers in the lung is related most directly to fiber diameter decrease and, perhaps, the formation of leached layers. An in-vitro technique should measure these parameters directly rather than infer them from other measurements.

b) Experimental simplicity: Laboratory and computational procedures should be as simple as possible and the same for all fiber types regardless of dimension, geometry, or composition.

c) Isolated fiber model: To model the fiber environment thought to exist in the lung, an in-vitro technique should be designed so that dissolution products do not reach concentrations in solution high enough to influence the rate of dissolution.

d) Independence from other sample property measurements: The technique should not require additional sample property measurements, such as fiber diameter distribution or surface area, which are difficult to measure accurately and can introduce significant error.

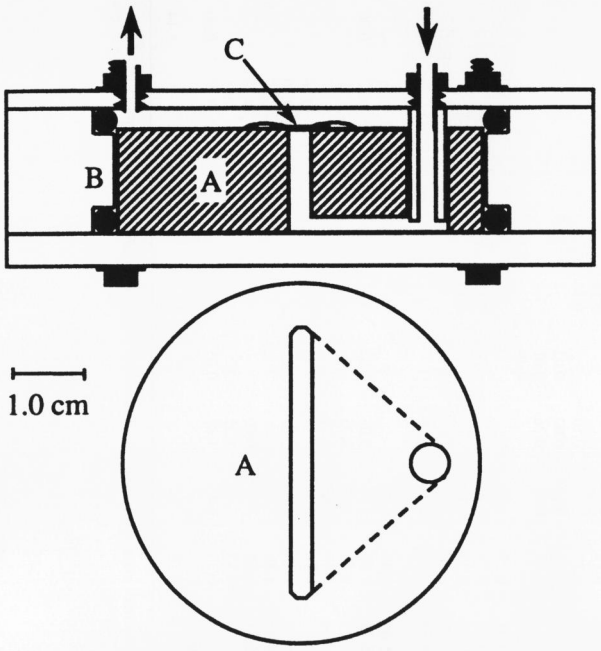


Figure 1. A cross-sectional view of the fibers (C) and mount (A) in place in the cell (B) and a planar view of the mount without fibers.

e) Direct application to in-vivo samples: Direct measurement of samples used for in-vivo studies is preferable to inferring rates for these samples from measurements on differently-prepared material from the same sample or on a different sample of similar composition.

f) Rapidity and low-cost: The technique should be quick and inexpensive.

This paper describes an in-vitro technique based on direct optical measurement of fiber diameter decrease which has been developed with these desirable criteria in mind.

## 2. Equipment and materials

The essential difference between the optical technique and other currently-used flow-through methods for measurement of fiber dissolution rate is in how the dissolution process is measured, not in the nature of the physiological fluid or the supporting equipment to maintain constant fluid flow and temperature. The optical method requires an appropriately-equipped optical microscope and suitably-designed sample holders. These holders can then be used with an existing flow-through system without essential change.

For the work reported here the physiological saline solution is a modified Gamble's solution having a pH near 7.4. The sample holders were maintained at 37 °C, the sample flow rates were generally in the range 0.2 to 0.3 ml/min. Details of the flow-through system have been published by Mattson [13].

The sample holders for the optical technique consist of a cylindrical mount and cell (figure 1). The fibers are attached to the mount with epoxy so that they span the slot. The mount is enclosed in the cell, which is held together by four bolts and sealed with O-rings at top and bottom. During a run, 1.5 cm long pieces of rubber tubing are attached to the lower bolt heads on the outflow side of the cell to tilt it so that bubbles are removed.

The measurement device is an optical microscope with a 40x, 8 mm focal length, 0.5 numerical aperture objective and a 16X digital filar ocular. This provides direct observation of the fiber during measurement, which is essential to obtain accurate, reproducible fiber diameters. Standard video measuring equipment gave diameter measurements which varied unreproducibly with brightness of the microscope field of view, video gain, and fiber characteristics.

Table 1 contains details of the fibers included in this study, which were produced, free of binder or other organic coatings, by a variety of commercial or laboratory processes. The chemical compositions were measured using standard techniques (X-ray fluorescence, inductively-coupled plasma, atomic absorption, and various wet chemical techniques) on either the bulk glass from which the fibers were made or on the fibers themselves. In the case of a few samples, the reported analysis is that of a different fiber sample formed from the same bulk glass. Several fiber compositions in table 1, which are well-known in the fiber dissolution literature, are identified by name in the table. These are not necessarily samples of the identical material studied elsewhere.

## 3. Measurement procedure

### 3.1 Sample pretreatment

Binder or other organic coatings such as oil can, if desired, be removed by low-temperature ashing in oxygen plasma. Removal by heat treatment may change the annealing state of the fibers and should be avoided.

### 3.2 Fiber mounting

Fibers can generally be pulled by hand directly from the original sample and mounted individually. Typically these fibers will be larger in diameter than the average of the original sample since the larger diameter fibers tend to be longer and easier to see and to work with. No attempt was made to pull fibers representative of the average fiber diameter, although this could be done. The fibers are mounted by applying a layer of epoxy resin to the top surface of the mount on either side of the slot and placing eight to ten individual fibers at about equal intervals along the slot. Each fiber should span the slot and be immersed in the epoxy on each side.

For samples which have been processed for shot removal, to isolate a respirable fraction, or for some other reason, it may not be possible to handle fibers individually due to their short length or small diameter. In this case about 2 mg of fibers are dispersed in about 5 ml of deionized water by ultrasonic treatment. The fibers are

Table 1. Source and chemical compositional data for the fiber samples

| sample no. | sample name | fiber source | preprocessing | analysis source | oxide chemical composition in wt% | | | | | | | | | | | | | | | |
|---|---|---|---|---|---|---|---|---|---|---|---|---|---|---|---|---|---|---|---|---|
| | | | | | $SiO_2$ | $Al_2O_3$ | CaO | MgO | $Na_2O$ | $K_2O$ | $B_2O_3$ | FeO | $Fe_2O_3$ | $TiO_2$ | $SO_3$ | SrO | BaO | $F_2$ | $P_2O_5$ | MnO | $ZrO_2$ |
| 1 | 7753 | laboratory continuous fiber | none | g | 66.03 | 0.63 | 5.90 | 3.08 | 15.64 | 0.81 | 7.66 | | 0.35 | 0.12 | | | | | | | |
| 2 | B-01 | laboratory continuous fiber | none | g | 61.33 | 0.11 | 16.28 | 3.44 | 15.12 | 0.41 | 3.00 | | 0.23 | 0.11 | | | | | | | |
| 3 | MMVF11 | laboratory continuous fiber | none | g | 63.64 | 3.95 | 7.36 | 2.93 | 15.71 | 1.38 | 4.28 | | 0.32 | | 0.18 | | | | | | |
| 4 | MMVF10 | laboratory continuous fiber | none | g | 57.15 | 5.43 | 7.82 | 4.25 | 15.11 | 1.07 | 8.63 | | 0.10 | | | | | 0.76 | | | |
| 5 | MMVF10 | production glass wool | respirable separate | f | 57.50 | 5.10 | 7.50 | 4.13 | 14.95 | 1.06 | 8.75 | | 0.07 | 0.01 | 0.12 | | | 0.83 | | | |
| 6 | MMVF10a | production glass wool | respirable separate | f | 57.21 | 5.10 | 7.17 | 4.48 | 15.64 | 1.04 | 8.40 | | 0.05 | 0.01 | 0.00 | 0.00 | 0.01 | 0.36 | | | 0.02 |
| 7 | NK8340 | laboratory continuous fiber | none | g | 64.93 | 2.12 | 9.10 | 3.08 | 14.59 | 0.51 | 4.63 | 0.12 | 0.37 | | 0.14 | | | | | | |
| 8 | NK8340 | production glass wool | blended | f | 64.92 | 2.12 | 9.08 | 3.03 | 14.56 | 0.51 | 4.66 | 0.12 | 0.38 | | 0.15 | 0.10 | | | | | |
| 9 | | laboratory continuous fiber | none | g | 66.49 | 0.60 | 8.43 | 2.82 | 15.33 | 0.12 | 5.48 | 0.17 | 0.22 | | 0.15 | | | | | | |
| 10 | | production glass wool | blended | f | 66.61 | 0.61 | 8.41 | 2.77 | 15.48 | 0.12 | 5.44 | 0.19 | 0.20 | | 0.16 | | | | | | |
| 11 | | laboratory continuous fiber | none | s | 66.51 | 0.66 | 8.95 | 2.87 | 14.94 | 0.32 | 5.36 | | 0.13 | | | | 0.11 | | | | |
| 12 | | laboratory glass wool | none | f | 66.51 | 0.66 | 8.95 | 2.87 | 14.94 | 0.32 | 5.36 | | 0.13 | | | | 0.11 | | | | |
| 13 | | laboratory continuous fiber | none | s | 62.78 | 0.88 | 8.69 | 2.57 | 14.33 | 0.40 | 9.94 | | 0.17 | | | | | | | | |
| 14 | | laboratory continuous fiber | none | s | 62.78 | 0.88 | 8.69 | 2.57 | 14.33 | 0.40 | 9.94 | | 0.17 | | | | | | | | |
| 15 | | laboratory continuous fiber | none | s | 62.78 | 0.88 | 8.69 | 2.57 | 14.33 | 0.40 | 9.94 | | 0.17 | | | | | | | | |
| 16 | | laboratory continuous fiber | none | s | 62.78 | 0.88 | 8.69 | 2.57 | 14.33 | 0.40 | 9.94 | | 0.17 | | | | | | | | |
| 17 | | laboratory continuous fiber | none | s | 62.78 | 0.88 | 8.69 | 2.57 | 14.33 | 0.40 | 9.94 | | 0.17 | | | | | | | | |
| 18 | | laboratory glass wool | none | f | 62.78 | 0.88 | 8.69 | 2.57 | 14.33 | 0.40 | 9.94 | | 0.17 | | | | | | | | |
| 19 | | laboratory glass wool | none | f | 62.60 | 0.93 | 8.71 | 2.58 | 14.27 | 0.40 | 9.97 | | 0.13 | | | | | | | | |
| 20 | | laboratory continuous fiber | none | g | 63.29 | 1.05 | 9.12 | 2.54 | 14.28 | 0.51 | 8.74 | | 0.13 | | | | 0.15 | | | | |
| 21 | | laboratory glass wool | none | f | 63.49 | 1.03 | 9.12 | 2.59 | 14.09 | 0.49 | 8.47 | | 0.22 | | 0.10 | | 0.14 | | | | |
| 22 | | laboratory continuous fiber | none | f | 47.35 | 3.19 | 6.66 | 2.60 | 19.06 | 0.01 | 19.18 | | 0.03 | 0.01 | 0.02 | 0.02 | | 3.09 | | | |
| 23 | | laboratory continuous fiber | none | f | 53.17 | 5.09 | 8.82 | 4.99 | 20.62 | 0.57 | 6.07 | | 0.18 | 0.07 | 0.26 | 0.01 | | | | | |
| 24 | | laboratory continuous fiber | none | g | 50.04 | 8.08 | 11.25 | 1.52 | 4.94 | 0.07 | 23.35 | | | | | 0.49 | | | | | |
| 25 | | laboratory continuous fiber | none | g | 56.64 | 1.10 | 7.61 | 2.72 | 14.62 | 0.82 | 16.25 | 0.04 | 0.25 | 0.13 | | | | | | | |
| 26 | | laboratory continuous fiber | none | g | 56.56 | 1.07 | 7.40 | 2.65 | 14.22 | 0.78 | 12.91 | 0.06 | 0.19 | 0.13 | | | 4.15 | | | | |
| 27 | | laboratory continuous fiber | none | g | 56.47 | 1.08 | 7.15 | 2.55 | 13.92 | 0.74 | 9.54 | 0.06 | 0.20 | 0.12 | | | 8.10 | | | | |
| 28 | | laboratory continuous fiber | none | f | 47.31 | 7.40 | 12.25 | 2.09 | 5.91 | 0.80 | 23.04 | 0.11 | 0.10 | | | 0.54 | | | | | |
| 29 | | laboratory rock wool | none | f | 40.94 | 21.74 | 16.41 | 11.62 | 0.83 | 0.91 | | 4.59 | 1.06 | 1.71 | | | | | | | |
| 30 | 607 | production rock wool | respirable separate | f | 58.30 | 1.25 | 38.70 | 0.40 | 0.30 | 0.10 | | | 0.10 | 0.05 | | | | | 0.05 | | |
| 31 | MMVF34 | production rock wool | shot removed | f | 38.54 | 22.95 | 15.18 | 10.22 | 1.69 | 0.78 | | 5.66 | 0.97 | 1.95 | | | | | 0.37 | 0.31 | |
| 32 | MMVF34 | production rock wool | respirable separate | f | 38.84 | 22.99 | 15.13 | 10.41 | 1.68 | 0.81 | | 5.28 | 1.60 | 1.96 | 0.08 | 0.05 | 0.04 | | 0.41 | 0.32 | 0.06 |
| 33 | FI980889 | production rock wool | none | s | 45.59 | 14.92 | 14.28 | 11.10 | 2.01 | 1.03 | | 7.07 | 0.58 | 1.59 | 0.35 | | | | 0.40 | 0.18 | |
| 34 | FI980890 | production rock wool | none | s | 39.88 | 20.61 | 13.54 | 11.49 | 1.57 | 0.83 | | 6.64 | 0.59 | 1.63 | 0.29 | | | | 0.34 | 0.17 | |
| 35 | QFHA19 | production rock wool | shot removed | f | 40.14 | 18.91 | 19.12 | 11.57 | 1.77 | 0.45 | | 4.62 | 0.81 | 1.58 | | | | | | 0.16 | |
| 36 | QFHA22 | production rock wool | blended | f | 41.62 | 21.62 | 15.56 | 9.83 | 1.72 | 0.43 | | 5.54 | 1.15 | 1.65 | | | | | | 0.16 | |
| 37 | QFHA23 | production rock wool | blended | f | 39.53 | 21.92 | 16.76 | 11.01 | 1.94 | 0.43 | | 4.95 | 1.36 | 1.64 | | | | | | 0.17 | |
| 38 | QFHA25 | production rock wool | blended | f | 38.26 | 22.73 | 25.19 | 6.58 | 0.74 | 0.39 | | 3.38 | 0.64 | 1.17 | 0.60 | | | | | 0.17 | |
| 39 | MMVF22 | production slag wool | none | f | 38.11 | 10.97 | 37.86 | 10.41 | 0.40 | 0.47 | | | 0.37 | 0.45 | 1.25 | | | | | 0.68 | |
| 40 | MMVF22 | production slag wool | respirable separate | f | 38.35 | 10.55 | 37.50 | 9.90 | 0.38 | 0.45 | | | 0.30 | 0.45 | 1.81 | 0.05 | 0.04 | | | 0.70 | 0.06 |
| 41 | 1260C | production high-temperature wool | none | f | 76.43 | 1.59 | 0.40 | 20.39 | 0.16 | 0.22 | 0.08 | 0.28 | 0.12 | | | | | | | | |
| 42 | | production high-temperature wool | none | f | 63.99 | 0.56 | 16.39 | 13.45 | 0.08 | 0.08 | | | 0.16 | | | | | | | | 5.14 |

Note: Chemical analysis source: f = on the fiber sample; g = on the bulk glass from which fiber was formed; s = on a different fiber sample formed from the same bulk glass. If no value is reported for FeO, total iron is reported as $Fe_2O_3$.
Total sulfur is reported as $SO_3$.
Analysis on no. 30 is taken from [4].

filtered onto a 45 mm diameter membrane filter and allowed to dry thoroughly. A very thin layer of epoxy resin is applied to the top surface of the mount on either side of the slot and allowed to cure to a tacky stage. The mount is turned upside down and pressed gently onto the fibers on the filter. The filter is then gently peeled off and discarded. This will leave many fibers adhered to the epoxy and sticking out over the slot in the mount. After the epoxy has cured, a binocular microscope is used to identify ten to twelve fibers which are good candidates for measurement due to their smooth, uniform diameter, good adherence to the mount, and clear visibility in the slot. These fibers are marked by a small spot of colored nail polish as close as possible to them on the mount.

### 3.3 Starting a run

The mount is loaded into the cell as shown in figure 1 and filled by syringe with simulated lung fluid at room temperature. The initial diameter of each fiber is measured using the diameter measurement procedure given below. The flow lines are connected to the cell, the tubing feet are placed on the bolt heads on the cell bottom at the outflow side of the cell, and the cell is placed into the constant temperature bath.

### 3.4 Fiber diameter measurement

Typically, a production fiber can change diameter significantly even within a single microscope field of view (170 µm). It is therefore essential that successive diameter measurements be made at the same place on any given fiber. This is most easily accomplished by measuring the diameter at a set distance (1/2 the field of view, for example) from the edge of the slot. No reduction in dissolution rate has generally been found at the slot edge even though a stagnant layer might be expected there, but it is good practice to check for this during a run.

The ideal image for measurement depends to some degree on the fiber diameter and whether the dissolution is congruent or incongruent. It probably also depends on the particular microscope design. The author's experience indicates the following guidelines:

a) Congruent dissolution: When the focal plane is just below the optimum position for measurement, the fiber appears dark at the edges, grading to light in the center. As the focal plane is raised, the lighter, central portion of the fiber expands, and two dark bands appear along the edges yielding the image shown in figure 2a. Often, particularly with smaller diameter fibers, there is a blue tinge outside of these bands. As the focal plane is raised further, the two bands lighten and become tinged with yellow. For fibers greater than about 4 µm in diameter, the image diameter is the same throughout this change in focal plane, but for fibers less that about 4 µm in diameter, the image diameter changes. The true fiber diameter is always the distance between the outer edges of the dark bands as shown in figures 2a and b just before they become tinged with yellow. When the fiber diameter is smaller than about 2 µm, it may yield a sharply defined image like the images of figures 2a and b, but often the dark bands are absent, and the best image is that shown in figure 2c, in which the fiber is uniformly dark.

b) Incongruent dissolution: A leached-layer on an unaltered fiber core could be detected and measured only if the layer was thicker than about 1 µm. At some positions of the focal plane most fibers show structures which appear to be leached layers but are not. It is good practice, when fibers are first immersed in the solution, to observe several as the focal plan is raised and lowered to identify structures which could be mistaken for a leached layer. The appearance of leached layers varies, depending on how much material has been leached from the layer, from barely distinguishable from the fluid to barely distinguishable from the unaltered core. The image in figure 2d is of a highly leached layer which tends toward the former. The outer leached diameter is measured in a way similar to that of congruent fibers – by raising the focal plane through that level which makes the outer part of the fiber as dark as possible until it just begins to lighten. The true diameter of the leached layer is then the distance between the outer edges of the darker area. The best image for measuring the core is when it first presents a clearly defined boundary with the leached layer as the focal plane is raised. If the leached layer is highly leached, it may never be dark enough to obscure the core. This is the case in figure 2d, which shows a good image for measuring both the leached layer and the core. If the leached layer is only slightly leached, the core may not appear until the focal plane is raised further after measuring the leached layer. The lower relief of the leached material, particularly after complete leaching, is good confirmation that a leached layer was measured rather than some other structure.

### 3.5 Frequency of measurement

Typically, it is not necessary to plan a set measurement schedule, but rather to start with daily measurements and then lengthen the time interval as necessary until there is a 0.5 to 1.0 µm difference in diameter between subsequent measurements (or less if the initial diameters of the fibers are near 2 µm). This interval is then continued until the fibers are completely dissolved, too many fibers are broken or unmeasurable in some way, or the fibers have been measured at enough times to define the dissolution rate with confidence. The data do not define a clear, consistent point (such as a diameter decrease of 2 µm, for example) at which such confidence is generally possible, so it is advisable to follow the dissolution as far as time constraints allow.

The cooling of the cell during the measuring process sets an upper limit to the frequency at which diameter measurements can be made without introducing significant error into the calculated dissolution rate due to time

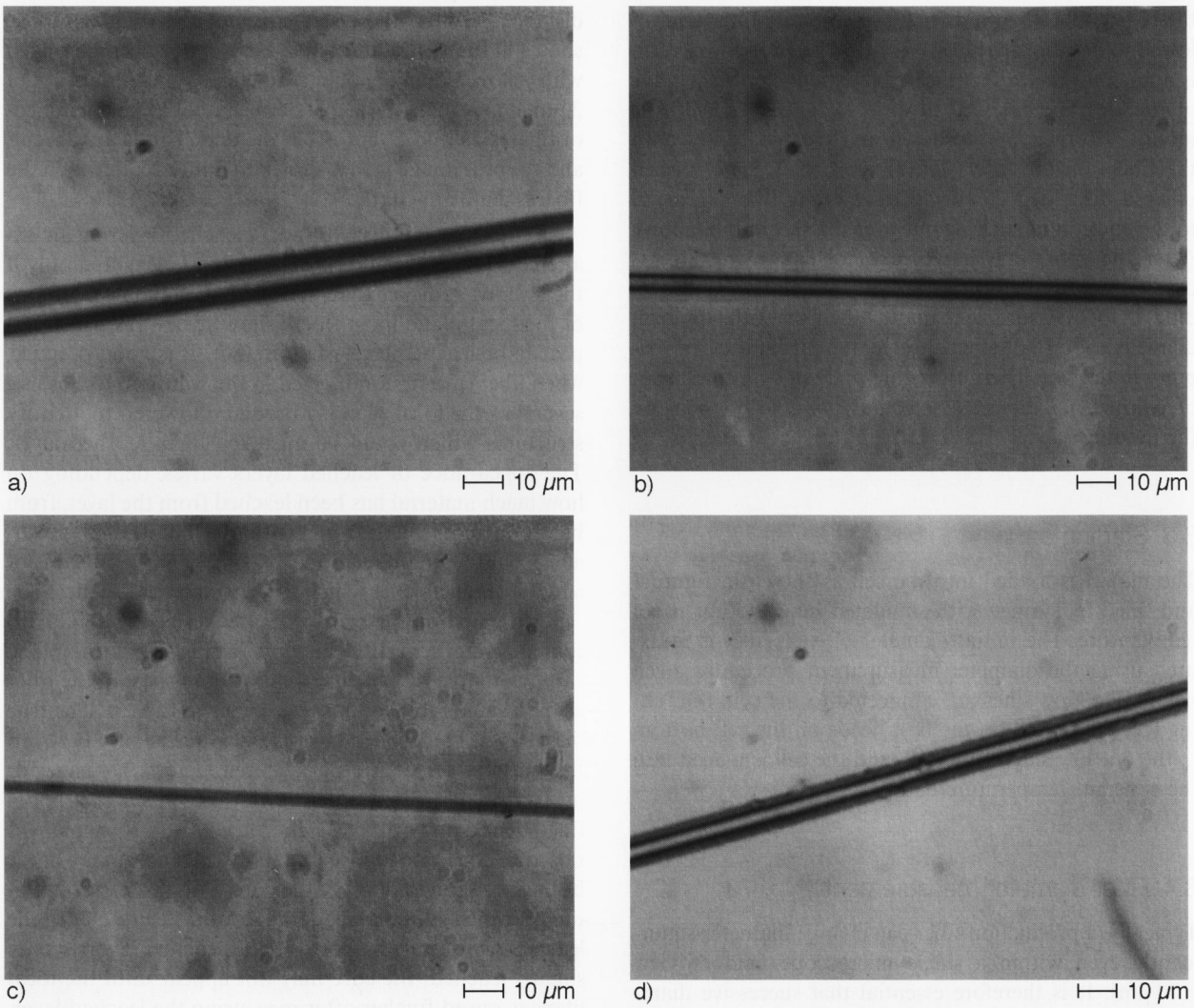


Figures 2a to d. Micrographs typical of fibers for diameter measurement; a) congruently-dissolving fiber about 10 μm in diameter, b) congruently-dissolving fiber about 4 μm in diameter, c) congruently-dissolving fiber about 2 μm in diameter, d) incongruently-dissolving fiber showing the unaltered core surrounded by a leached layer.

at reduced temperature. Cell temperature measurements during the fiber diameter measurement and subsequent reheating of the cell in the water bath together with published data on the effect of temperature on fiber dissolution rate [10] allow an estimate of this error. For a typical measurement time of 20 min, 3 % error in the dissolution rate corresponds to about three measurements per day, which is not a serious limitation even for the most rapidly dissolving fibers.

### 3.6 Ending a run

At the end of a run, if SEM data are desired to confirm the optical measurements or to define the thickness of a leached layer, the cell should be taken apart while completely immersed in water, and the mount lifted vertically through the water surface to minimize stress on the fibers. A few drops of ethanol put on the water surface near the fibers just before they break the surface will also help prevent fiber breakage by reducing surface tension. For SEM examination the mount should be embedded in epoxy and a polished cross-section made as nearly as possible at the point the fibers were measured optically.

### 3.7 Calculations

In this paper congruent fiber dissolution rate is expressed as dissolution time, $t_{dis}$, the time in days to dissolve a 1 μm diameter fiber. This parameter has the advantage of expressing directly the biologically relevant aspect of dissolution [22]. Furthermore, $t_{dis}$ can be calculated from the optical data by a simple equation which depends on no other properties of the fiber or fiber sample:

$$t_{dis} = \frac{t}{d_0 - d} = \frac{t}{\Delta d} = \frac{1}{m} . \quad (1)$$

The slope, $m$, is obtained by least-squares' analysis of the change of $\Delta d$ with time, and $t_{dis}$ is calculated from the slope. The least-squares' analysis does not force the line to pass through the origin since the initial measurement is not necessarily more accurate than any subsequent one.

For incongruently-dissolving fibers it is not yet known whether biopersistence depends on leaching rate only, on total dissolution rate only, or on some combination of both. For this reason it is useful to define a leaching time, $t_l$, the time in days for a 1 µm diameter fiber to be completely leached, and a total dissolution time, $t_n$, the time in days for a 1 µm diameter to be completely dissolved. They are given by equations similar to equation (1), where $d$ is the diameter of the unaltered core for $t_l$, and $d$ is the outer diameter of the leached layer for $t_n$. They are evaluated in a manner analogous to $t_{dis}$.

For congruently dissolving fibers, $k_{dis}$ in ng/(cm$^2$ h) is approximately equal to $5000/t_{dis}$ [22]. The exact relationships between $k_{dis}$ and the dissolution times are:

$$k_{dis} \equiv \frac{10^5 \cdot \varrho}{24 \cdot 2 \cdot t_{dis}} \tag{2}$$

for congruently-dissolving fibers. And:

$$k_{dis} \cong \frac{10^5 \cdot \varrho}{24 \cdot 2} \left( \frac{X_l}{t_l} + \frac{1-X_l}{t_n} \right) \tag{3}$$

for incongruently-dissolving fibers. The factor 2 in the denominator of equations (2) and (3) reflects the fact that the decrease in fiber diameter is twice the dissolution velocity. The mass fraction leached, $X_l$, is defined equal to 0 for congruent dissolution. By this convention congruent dissolution is a special case of incongruent dissolution with $t_{dis}$ equated to $t_n$. Generally, for incongruent dissolution, $X_l$ will not be known, and $k_{dis}$ can be only estimated from the diameter decrease. For many compositions the mass fraction of $SiO_2+Al_2O_3$ is a rough upper limit to $X_l$.

## 4. Results and discussion

Table 2 summarizes the results of $t_{dis}$ measurement by the optical method and by the methods of mass loss, solution analysis, and SEM fiber diameter measurement. The latter three methods have been described elsewhere [10 and 13]. For the mass loss and solution analysis methods, values for $t_n$ and $t_l$ are calculated only for those samples for which the rate of mass loss with time (measured directly or calculated from solution analysis) shows a clear break attributable to complete leaching of the fibers. Only when this break is apparent in the data, is it possible to determine unambiguously both the leaching and total dissolution. Thus, for example, a single, congruent dissolution rate is reported from the mass loss and solution analysis methods for sample no. 4 even though SEM analysis shows the dissolution to be incongruent. The initial fiber diameter data in table 2 are for the mounted fibers only and do not necessarily reflect the average fiber diameter of the sample.

### 4.1 Validity of the dissolution model

The data in table 2 indicate that the standard error associated with a linear fit to the data for a single measurement of $t_{dis}$ by the optical method is typically less than about 10 % of the measured value. Most of the instances of larger standard error are the result of small initial fiber diameter, which limits the number of measured points and the accuracy of each measurement. For incongruently dissolving fibers, the standard error in both $t_n$ and $t_l$ is typically less than about 15 %, which reflects the greater complexity of the optical image. Thus, the model of constant diameter decrease with time is in general a good one for both congruent and incongruent fiber dissolution.

Although the dissolution process is essentially a linear diameter decrease with time, there are some departures from strict linearity which may be significant to details of the dissolution process. Figure 3 shows diameter decrease data for a range of $t_{dis}$ values together with the linear fits to the data by least-squares' analysis. The dissolution of samples no. 2 and no. 30 are strictly linear, which is the case for the majority of fibers. Some fiber samples, such as no. 31, show an initial period of slower dissolution. This may relate to the presence of a thin surface layer on the fibers from which the more volatile components have been partially removed during the fiberization process as discussed by Bauer [23] and by Mattson [24]. Typically, this is a small part of the dissolution process both in terms of time and in terms of the amount of fiber dissolved. Some fibers, such as no. 8, show an initial period of more rapid dissolution. This has been found primarily with production of mineral wool samples. This initial rapid dissolution can last for weeks through a diameter decrease of several micrometers, so it is unlikely to be related to a surface effect. It may relate to leached layers which are not recognizable optically.

### 4.2 Reproducibility

Table 2 contains data for replicate runs for a number of samples and the standard deviation of the dissolution times of these replicate runs expressed as a percent of the mean value. This standard deviation is typically less than about 20 % for both congruent and incongruent dissolution. Higher values are the result of too few diameter measurements because the dissolution process was not followed far enough (a total diameter decrease of 0.4 µm for the second run of sample no. 33, and 0.8 µm for the second run of sample no. 29) or was not measured frequently enough (only one measurement of unaltered core diameter for each of the runs of sample no. 22).

Table 2. Dissolution time data for the fiber samples (for units of $d_0$, $\varrho$, $t_{dis}$, $t_n$, $t_l$, see section 5).

| sample | sample | $d_0$ | | $\varrho$ | optical method | | | | | | | | | mass loss method | | | | solution analysis method | | | | SEM method | | | | | |
|---|---|---|---|---|---|---|---|---|---|---|---|---|---|---|---|---|---|---|---|---|---|---|---|---|---|---|---|
| | | | | | $t_{dis}$ | | | $t_n$ | | | $t_l$ | | | $t_{dis}$ | | $t_n$ | $t_l$ | $t_{dis}$ | | $t_n$ | $t_l$ | $t_{dis}$ | | $t_n$ | | $t_l$ | |
| no. | name | value | $\sigma$ | value | value | stderr | $\sigma$ in % | value | stderr | $\sigma$ in % | value | stderr | $\sigma$ in % | value | stderr | value | value | value | stderr | value | value | value | stderr | value | stderr | value | stderr |
| 1 | 7753 | 11.99 | 0.19 | 2.47 | 5.57 | 0.24 | 4 | | | | | | | 5.88 | 0.68 | | | 6.00 | 1.38 | | | 5.56 | 0.25 | | | | |
| 1 | | 10.62 | 0.39 | 2.47 | 5.24 | 0.09 | | | | | | | | | | | | | | | | | | | | | |
| 2 | B-01 | 9.52 | 0.30 | 2.60 | 0.76 | 0.03 | | | | | | | | 0.97 | 0.04 | | | | | | | 1.02 | 0.02 | | | | |
| 3 | MMVF11 | 10.59 | 0.06 | 2.48 | 37.79 | 0.88 | | | | | | | | 66.75 | 4.48 | | | 61.73 | 3.69 | | | 38.44 | 0.72 | | | | |
| 4 | MMVF10 | 14.19 | 0.13 | 2.51 | 28.41 | 0.99 | | | | | | | | 39.02 | 5.24 | | | 43.58 | 9.08 | | | | | 29.45 | 3.34 | 22.27 | 1.91 |
| 5 | MMVF10 | 2.46 | 0.08 | 2.55 | 11.79 | 2.24 | | | | | | | | 23.52 | 1.70 | | | 20.01 | 1.29 | | | | | | | | |
| 6 | MMVF10a | 2.30 | 0.06 | 2.55 | 13.78 | 3.52 | | | | | | | | 18.95 | 0.71 | | | | | 37.50 | 9.83 | | | | | | |
| 7 | NK8340 | 10.25 | 0.09 | 2.50 | 18.95 | 0.65 | | | | | | | | 19.96 | 0.92 | | | | | | | | | | | | |
| 8 | NK8340 | 6.55 | 0.43 | 2.50 | 20.50 | 0.69 | | | | | | | | 19.80 | 1.32 | | | | | | | | | | | | |
| 9 | | 10.04 | 0.05 | 2.50 | 7.41 | 0.22 | | | | | | | | 8.74 | 0.66 | | | | | | | | | | | | |
| 10 | | 6.35 | 1.07 | 2.49 | 7.69 | 0.41 | | | | | | | | 7.78 | 0.29 | | | | | | | | | | | | |
| 11 | | 10.03 | 0.03 | 2.54 | 7.32 | 0.38 | | | | | | | | 7.12 | 0.29 | | | | | | | | | | | | |
| 12 | | 4.58 | 0.47 | 2.54 | 7.68 | 0.42 | | | | | | | | 10.74 | 0.53 | | | | | | | | | | | | |
| 13 | | 10.23 | 0.06 | 2.49 | 1.63 | 0.10 | | | | | | | | 2.02 | 0.14 | | | | | | | | | | | | |
| 14 | | 3.32 | 0.06 | 2.49 | 2.57 | 0.41 | 14 | | | | | | | 1.83 | 0.31 | | | | | | | | | | | | |
| 14 | | 3.37 | 0.04 | 2.49 | 2.11 | 0.53 | | | | | | | | | | | | | | | | | | | | | |
| 15 | | 6.65 | 0.10 | 2.49 | 1.63 | 0.11 | 16 | | | | | | | 1.91 | 0.10 | | | | | | | | | | | | |
| 15 | | 6.79 | 0.06 | 2.49 | 1.31 | 0.07 | | | | | | | | | | | | | | | | | | | | | |
| 15 | | 7.01 | 0.04 | 2.49 | 1.14 | 0.11 | | | | | | | | | | | | | | | | | | | | | |
| 15 | | 7.08 | 0.04 | 2.49 | 1.57 | 0.16 | | | | | | | | | | | | | | | | | | | | | |
| 16 | | 9.43 | 0.07 | 2.49 | 1.31 | 0.05 | 22 | | | | | | | 1.85 | 0.14 | | | | | | | | | | | | |
| 16 | | 9.19 | 0.05 | 2.49 | 1.94 | 0.27 | | | | | | | | | | | | | | | | | | | | | |
| 16 | | 9.46 | 0.05 | 2.49 | 1.39 | 0.11 | | | | | | | | | | | | | | | | | | | | | |
| 17 | | 2.74 | 0.05 | 2.49 | 1.83 | 0.20 | | | | | | | | | | | | | | | | | | | | | |
| 18 | | 5.81 | 0.33 | 2.48 | 1.59 | 0.07 | | | | | | | | 5.06 | 0.43 | | | | | | | | | | | | |
| 19 | | 5.57 | 0.40 | 2.48 | 1.64 | 0.09 | | | | | | | | 4.29 | 0.20 | | | | | | | | | | | | |
| 20 | | 10.21 | 0.06 | 2.49 | 2.66 | 0.10 | | | | | | | | 3.17 | 0.13 | | | | | | | | | | | | |
| 21 | | 7.23 | 0.67 | 2.49 | 2.36 | 0.12 | | | | | | | | 4.08 | 0.18 | | | | | | | | | | | | |
| 22 | | 9.53 | 0.10 | 2.52 | | | | 0.92 | 0.03 | 1 | 0.21 | 0.00 | 106 | | | | | 0.19 | 0.02 | | | | | 0.78 | 0.31 | 0.10 | 0.03 |
| 22 | | 9.24 | 0.03 | 2.52 | | | | 0.91 | 0.03 | | 0.03 | 0.00 | | | | | | | | | | | | | | | |
| 23 | | 9.51 | 0.18 | 2.59 | | | | 1.94 | 0.07 | 1 | 1.27 | 0.11 | 2 | | | 2.52 | 0.47 | | | | | | | 1.76 | 0.20 | 1.07 | 0.09 |
| 23 | | 9.83 | 0.07 | 2.59 | | | | 1.91 | 0.12 | | 1.31 | 0.13 | | | | | | | | | | | | | | | |
| 23 | | 10.06 | 0.07 | 2.59 | | | | 1.91 | 0.10 | | 1.25 | 0.10 | | | | | | | | | | | | | | | |
| 24 | | 10.86 | 0.09 | 2.39 | | | | 3.22 | 0.60 | 22 | 0.60 | 0.04 | 35 | | | 2.41 | 0.51 | | | 3.46 | 0.53 | | | | | | |
| 24 | | 10.88 | 0.15 | 2.39 | | | | 3.60 | 0.32 | | 0.46 | 0.04 | | | | | | | | | | | | | | | |
| 24 | | 10.27 | 0.13 | 2.39 | | | | 4.89 | 0.52 | | 0.91 | 0.02 | | | | | | | | | | | | | | | |
| 25 | | 11.12 | 0.07 | 2.49 | | | | 0.31 | 0.02 | 21 | 0.13 | 0.02 | 23 | 0.24 | 0.03 | | | | | | | | | 0.28 | 0.02 | 0.20 | 0.01 |
| 25 | | 9.56 | 0.05 | 2.49 | | | | 0.40 | 0.05 | | 0.13 | 0.01 | | | | | | | | | | | | | | | |
| 25 | | 9.79 | 0.04 | 2.49 | | | | 0.42 | 0.03 | | 0.19 | 0.02 | | | | | | | | | | | | | | | |
| 25 | | 10.15 | 0.05 | 2.49 | | | | 0.44 | 0.04 | | 0.19 | 0.02 | | | | | | | | | | | | | | | |
| 25 | | 9.79 | 0.06 | 2.49 | | | | 0.60 | 0.06 | | 0.24 | 0.03 | | | | | | | | | | | | | | | |
| 25 | | 9.56 | 0.04 | 2.49 | | | | 0.52 | 0.04 | | 0.16 | 0.02 | | | | | | | | | | | | | | | |
| 25 | | 9.40 | 0.06 | 2.49 | | | | 0.42 | 0.05 | | 0.20 | 0.04 | | | | | | | | | | | | | | | |
| 26 | | 11.31 | 0.09 | 2.56 | | | | 0.39 | 0.02 | 28 | 0.23 | 0.08 | 21 | 0.33 | 0.02 | | | | | | | | | 0.37 | 0.04 | 0.28 | 0.02 |
| 26 | | 9.48 | 0.04 | 2.56 | | | | 0.58 | 0.06 | | 0.31 | 0.01 | | | | | | | | | | | | | | | |
| 27 | | 9.74 | 0.06 | 2.63 | | | | 0.65 | 0.08 | | 0.36 | 0.05 | | 0.48 | 0.04 | | | | | | | | | 0.65 | 0.01 | 0.50 | 0.01 |
| 28 | | 9.68 | 0.06 | 2.44 | | | | 1.61 | 0.33 | | 0.21 | 0.04 | | | | 1.83 | 0.20 | | | | | | | | | | |
| 29 | | 9.59 | 0.69 | 2.86 | 132.62 | 16.51 | 50 | | | | | | | 95.95 | 1.70 | | | 98.16 | 7.44 | | | | | | | | |
| 29 | | 14.26 | 2.39 | 2.86 | 62.97 | 3.63 | | | | | | | | | | | | | | | | | | | | | |
| 30 | 607 | 3.81 | 0.34 | 2.78 | 5.08 | 0.14 | | | | | | | | 7.60 | 0.25 | | | | | 8.53 | 1.76 | | | | | | |
| 31 | MMVF34 | 4.92 | 0.78 | 2.85 | 36.35 | 1.07 | | | | | | | | 60.65 | 7.80 | | | 67.47 | 7.21 | | | | | | | | |
| 32 | MMVF34 | 1.73 | 0.04 | 2.80 | 87.64 | 13.13 | | | | | | | | 66.12 | 3.98 | | | 79.27 | 7.62 | | | | | | | | |
| 33 | FI980889 | 4.61 | 0.23 | 2.79 | 199.45 | 48.04 | 29 | | | | | | | 307.54 | 35.80 | | | | | | | | | | | | |
| 33 | | 6.22 | 0.35 | 2.79 | 304.00 | 67.25 | | | | | | | | | | | | | | | | | | | | | |
| 34 | FI980890 | 6.49 | 0.46 | 2.82 | 67.27 | 5.38 | 11 | | | | | | | 132.02 | 13.10 | | | | | | | | | | | | |
| 34 | | 8.14 | 0.54 | 2.82 | 78.58 | 5.45 | | | | | | | | | | | | | | | | | | | | | |
| 35 | QFHA19 | 4.20 | 0.24 | 2.83 | 106.60 | 10.72 | | | | | | | | 83.75 | 6.19 | | | 106.81 | 11.42 | | | | | | | | |
| 36 | QFHA22 | 4.04 | 0.38 | 2.82 | 55.96 | 2.84 | | | | | | | | 55.37 | 0.42 | | | 73.90 | 2.04 | | | | | | | | |
| 37 | QFHA23 | 3.64 | 0.16 | 2.82 | 71.74 | 4.33 | | | | | | | | 47.84 | 3.31 | | | | | | | | | | | | |
| 38 | QFHA25 | 5.15 | 0.38 | 2.83 | 26.21 | 0.62 | | | | | | | | 31.99 | 0.29 | | | 48.97 | 3.42 | | | | | | | | |
| 39 | MMVF22 | 7.46 | 0.70 | 2.92 | 17.70 | 0.76 | | | | | | | | | | | | | | 14.17 | 0.24 | | | | | | |
| 40 | MMVF22 | 1.73 | 0.08 | 2.92 | 76.25 | 4.92 | | | | | | | | | | 71.73 | 7.71 | | | 58.77 | 6.63 | | | | | | |
| 41 | 1260C | 4.89 | 0.40 | 2.46 | 11.06 | 0.40 | | | | | | | | 19.64 | 0.98 | | | | | | | | | | | | |
| 42 | | 7.12 | 0.49 | 2.70 | 45.85 | 2.48 | | | | | | | | 46.64 | 1.08 | | | | | | | | | | | | |

Note: Fiber diameter data is for the mounted fibers only, not the original sample. – $\sigma$ = standard deviation of the fiber diameters in μm. – stderr = standard error of the linear fit to the data in an individual $t_{dis}$ dissolution rate determination. – $\sigma$ in % = standard deviation of multiple $t_{dis}$ dissolution rate determinations expressed as a percent of the mean value.

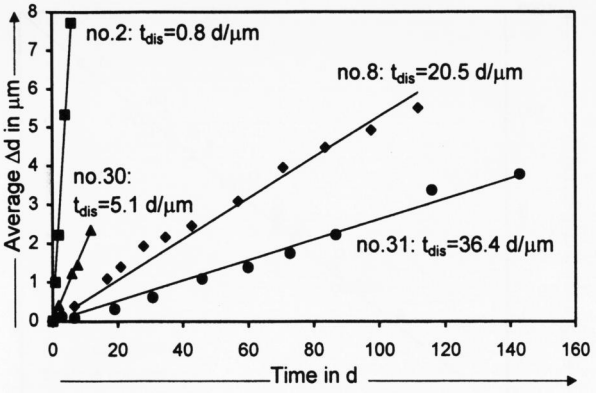


Figure 3. Typical optical data of fiber diameter decrease ($\Delta d$) with time. The four samples shown span the range of dissolution times measured.

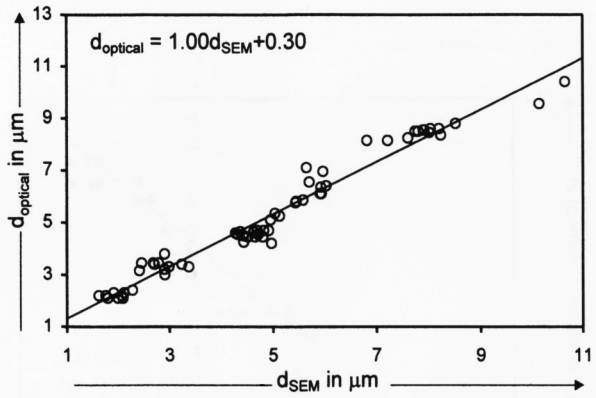


Figure 4. The correlation between optical and SEM diameter measurements of the same fibers. The line is a least-squares' fit.

## 4.3 Calibration of diameter measurements against SEM

In order to check the accuracy of the optical fiber diameter measurements, we measured the final fiber diameters by SEM for a number of completed runs. In all cases the fibers are from a continuous laboratory bushing, so that a small difference in the measurement position along the length of the fiber is not significant. Figure 4 shows a good correlation between the two diameter measurement techniques. The slope of the least squares' fit line is 1.00 with a slight offset indicating that the optical technique tends to yield a slightly larger diameter. This offset is small and, in any case, can have no effect on the dissolution rate calculated by the optical technique since the rate is based on diameter change.

## 4.4 Effect of flow rate

Sample no. 25 was used to examine the effect of flow rate since its very rapid incongruent dissolution should make it particularly sensitive to flow rate changes. The dissolution rate is significantly reduced under stagnant conditions but is independent of flow in the range studied and reported here, i.e. 0.06 to 0.40 ml/min. For convenience, the standard flow rate was set at 0.25 ml/min; it could certainly be reduced.

## 4.5 Effect of fiber diameter

The optical technique yields more accurate and reproducible dissolution rates when the initial fiber diameters are greater than about 2 µm since the measured fiber diameter changes can be larger and more points can be measured. This is also true of the mass loss and solution analysis methods due to poor dispersion of fine fibers in the mats [10 and 13]. It is therefore of general concern that measurements on larger diameter fibers be applicable to the dissolution of respirable fibers, which have diameters typically less than about 2 µm.

In most of the production fiber samples, the individual fibers measured by the optical technique span a large range of fiber diameters. In over half of these cases the dissolution times calculated from the individual fibers show a rough trend with dissolution time increasing with decreasing initial fiber diameter, particularly at diameters near 2 µm and below. The increase in dissolution time can be as much as a factor of 3. In addition, an increase in measured dissolution times sometimes occurs, regardless of initial fiber diameter, as individual fibers dissolve to diameters near 2 µm and below. This is true for both laboratory continuous fibers and for wool fibers. Fibers that have dissolved to diameters near 2 µm sometimes remain visible significantly beyond the time at which their earlier diameter change would predict complete congruent dissolution. The only evidence for a decrease in dissolution time with fiber diameter decrease is the larger dissolution time of sample no. 4 relative to sample nos. 5 and 6.

In general, one might expect that if there were any diameter effect, dissolution times would decrease rather than increase with fiber diameter since finer fibers would be cooled more rapidly and have, in consequence, more open structures. It is particularly hard to conceive of a process that would cause the small central portion of a large, congruently-dissolving fiber to dissolve more slowly than the rest of the fiber. The apparent correlation of dissolution rate to fiber diameter cannot be the result of systematic inaccuracies of the optical diameter measurement below about 2 µm. Figure 4 shows good agreement between optical and SEM diameter measurements. In addition, fibers sometimes remain visible long beyond the time of complete dissolution predicted from their earlier rate of diameter reduction.

To further examine the effect of diameter, continuous fibers samples (nos. 13 to 17) were produced at various diameters between 2.7 and 10.3 µm from a composition for which laboratory wool samples (no. 18 and no. 19) show a large effect of fiber diameter. The dissolution times measured by the optical method suggest little, if any, increase in dissolution rate for the smaller diameter fiber samples. Potential effects of fiber diameter on dis-

solution time remains an important, unresolved issue and the subject of continued investigation using the optical technique and other in-vitro methods.

## 4.6 Effect of forming and preprocessing

Table 1 contains a number of sets of fibers which are essentialy the same composition but differ in the forming process or sample preprocessing (nos. 4 to 21). These samples provide some idea of how such differences can affect the dissolution time of a given composition. For the optical technique, the variations within a compositional set are not significantly greater than the typical reproducibility of the measurement except for cases which include samples with an average initial fiber diameter of 2 to 3 μm. The large variation in these cases may relate, in part at least, to the limited number of measurements possible for the small diameter samples and the large uncertainty of each measurement. The mass loss and solution analysis data are more limited than the optical data, but the average variation for all the sets of similar compositions is about the same.

## 4.7 In-vitro method comparison

For congruently-dissolving fibers, figure 5 compares the dissolution times measured by the optical method with those measured by mass loss, solution analysis, and SEM. The agreement is good throughout the range. As expected from the SEM-optical comparison, dissolution times measured by the optical technique are within experimental error the same as those measured by SEM, falling close to the line indicating perfect agreement between the techniques. In almost all cases the dissolution times from the optical technique are less than or equal to those measured by mass loss or solution analysis. This probably relates to the isolated dissolution environment, which is characteristic of the optical and SEM methods, but which is difficult or impossible to achieve with the mass loss or solution analysis techniques.

For incongruently-dissolving fibers, figure 6 compares the total dissolution and leaching times measured by the optical method with those measured by mass loss, solution analysis, and SEM. The agreement is reasonable throughout the range of dissolution times. The greater scatter relative to figure 5 is partly the result of the scale of the graph, but it also reflects the greater complexity of the optical image and the assumptions involved in extracting $t_n$ and $t_l$ from the mass loss and solution analysis data. The data do not indicate any tendency for the optical and SEM dissolution times to be shorter than those derived from mass loss and solution analysis.

## 4.8 General conclusions

The optical method presented here provides a direct measure of the time it takes a fiber to dissolve in model physiological solutions. The method is conceptually and experimentally simple and applicable to all fiber types. It does not depend on other measurements such as fiber diameter distribution or surface area, which are known to introduce error and poor reproducibility in the standard mass loss and solution analysis methods. Nor does it rely on expensive instrumentation or extensive laboratory expertise such as that needed for chemical analysis. Because individual, isolated fibers are measured, a single flow rate gives for all fiber compositions the high surface area to flow conditions thought to exist in the lung. Although the technique produces the most accurate and reproducible results when applied to fibers in the 4 to 10 μm diameter range, it can be used to measure the dissolution rate of fibers as small as about 2 μm in diameter. The time for analysis is roughly proportional to the fiber dissolution time. For $t_{dis}$ near 50 d/μm, the optical technique takes about two months.

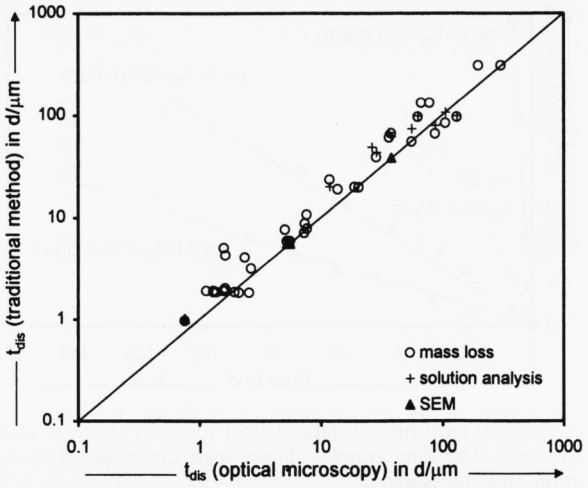


Figure 5. Comparison of dissolution times for congruently dissolving fibers measured by the optical method to those measured by traditional methods. The line indicates exact agreement between the methods.

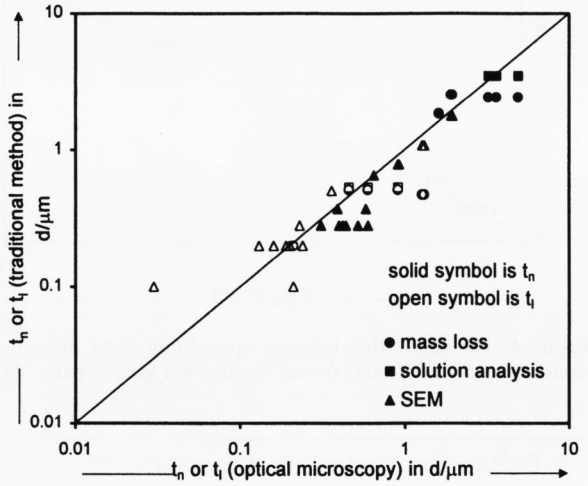


Figure 6. Comparison of dissolution times for incongruently dissolving fibers measured by the optical method to those measured by traditional methods. The line indicates exact agreement between the methods.

## 5. Nomenclature

$d$ = fiber diameter at time $t$ during dissolution in µm
$d_0$ = initial fiber diameter in µm
$d_{optical}$ = fiber diameter measured by the optical technique in µm
$d_{SEM}$ = fiber diameter measured by SEM in µm
$\Delta d$ = fiber diameter decrease: $d_0 - d$ in µm
$k_{dis}$ = fiber dissolution rate in ng/(cm² h)
$m$ = the slope in a plot of $\Delta d$ versus $t$
$\varrho$ = fiber density in g/cm³
$t$ = time in d
$t_{dis}$ = time to completely dissolve, congruently, a 1 µm diameter fiber in d/µm
$t_l$ = time to completely leach a 1 µm diameter fiber in d/µm
$t_n$ = time to completely dissolve, incongruently, a 1 µm diameter fiber in d/µm
$X_l$ = fraction of the initial mass leached during incongruent dissolution

*

Jon Bauer, Paul Boymel, Thomas Hanton, Martin Moore, and Thomas Steenberg provided fiber samples. Claire Hunkins and Cheryl Smith did most of the laboratory work which forms the basis of this paper. Walter Eastes and John Hadley provided guidance and critical review throughout the work. The author is grateful to all these colleagues for their support.

## 6. References

[1] Eastes, W.; Hadley, J. G.: Dissolution of fibers inhaled by rats. Inhal. Toxicol. **7** (1995) p. 179–196.
[2] Eastes, W.; Morris, K. J.; Morgan, A., et al.: Dissolution of glass fibers in the rat lung following intratracheal instillation. Inhal. Toxicol. **7** (1995) p. 197–213.
[3] Eastes, W.; Hadley, J. G.: A mathematical model of fiber carcinogenicity and fibrosis in inhalation and intraperitoneal experiments in rats. Inhal. Toxicol. **8** (1996) p. 323–343.
[4] Bernstein, D. M.; Morscheidt, C.; Grimm, H.-G., et al.: Evaluation of soluble fibers using the inhalation biopersistence model, a nine-fiber comparison. Inhal. Toxicol. **8** (1996) p. 345–385.
[5] Förster, H.: The behavior of mineral fibers in physiological solutions. In: Biological effects of man-made mineral fibers. Proc. WHO/IARC Conference, Copenhagen, 1982. Vol. 2. Copenhagen: World Health Organization, 1984. p. 27–59.
[6] Klingholz, R.; Steinkopf, B.: The reactions of MMMF in a physiological model fluid and in water. In: Biological effects of man-made mineral fibers. Proc. WHO/IARC Conference, Copenhagen, 1982. Vol. 2. Copenhagen: World Health Organization, 1984. p. 60–86.
[7] Leineweber, J. P.: Solubility of fibres in vitro and in vivo. In: Biological effects of man-made mineral fibers. Proc. WHO/IARC Conference, Copenhagen, 1982. Vol. 2. Copenhagen: World Health Organization, 1984. p. 87–101.
[8] Scholze, H.; Conradt, R.: An in-vitro study of the chemical durability of siliceous fibres. Ann. occup. Hyg. **31** (1987) no. 48, p. 683–692.
[9] Law, B. D.; Bunn, W. B.; Hesterberg, T. W.: Solubility of polymeric organic fibers and man-made vitreous fibers in Gambles solution. Inhal. Toxicol. **2** (1990) p. 321–339.
[10] Potter, R. M.; Mattson, S. M.: Glass fiber dissolution in a physiological saline solution. Glastech. Ber. **64** (1991) no. 1, p. 16–28.
[11] Bauer, J. F.; Law, B. D.; Hesterberg, T. W.: Dual pH durability studies of man-made vitreous fiber (MMVF). Environ. Health Perspect. **102** (1994) suppl. 5, p. 61–65.
[12] Meringo, A. de; Morscheidt, C.; Thélohan, S. et al.: In vitro assessment of biodurability: acellular systems. Environ. Health Perspect. **102** (1994) suppl. 5, p. 47–53.
[13] Mattson, S. M.: Glass fibres in simulated lung fluid: dissolution behavior and analytical requirements. Ann. occup. Hyg. **38** (1994) p. 857–877.
[14] Mattson, S. M.: Glass fiber dissolution in simulated lung fluid and measures needed to improve consistency and correspondence to in vivo dissolution. Environ. Health Perspect. **102** (1994) suppl. 5, p. 87–90.
[15] Thélohan, S.; Meringo, A. de: In vitro dynamic solubility test: influence of various parameters. Environ. Health Perspect. **102** (1994) suppl. 5, p. 91–96.
[16] Baillif, P.; Chouikhi, B.; Barbanson, L. et al.: Dissolution kinetics of glass fibres in saline solution: in vitro persistence of a sparingly soluble aluminum-rich leached layer. J. Mater. Sci. **30** (1995) p. 5691–5699.
[17] Guldberg, M.; Christensen, V. R.; Krøis, W. et al.: Method for determining in-vitro dissolution rates of man-made vitreous fibres. Glastech. Ber. Glass Sci. Technol. **68** (1995) no. 6, p. 181–187.
[18] Sebastian, K.: Comparitive in-vitro investigations of the chemical durability of inorganic fibrous materials. Glastech. Ber. Glass Sci. Technol. **68 C1** (1995) p. 215–222.
[19] Zoitos, B. K.; Meringo, A. de; Rouyer, E. et al.: In vitro measurement of fiber dissolution rate relevant to biopersistence at neutral pH: an interlaboratory round robin. Inhal. Toxicol. **9** (1997) p. 525–540.
[20] Guldberg, M.; Christensen, V. R.; Perander, M. et al.: Measurement of in-vitro fibre dissolution rate at acidic pH. Ann. occup. Hyg. **42** (1998) p. 233–243.
[21] Searl, A.; Buchanan, D.; Cullen, R. T. et al.: Biopersistence and durability of nine mineral fibre types in rat lungs over 12 months. Ann. occup. Hyg. **43** (1999) p. 143–153.
[22] Eastes, W.; Potter, R. M.; Hadley, J. G.: Estimating in-vitro glass fiber dissolution rate from composition. Inhal. Toxicol. in press.
[23] Bauer, J. F.: Effect of fiberization process on glass fiber surfaces. In: Clare, A. G.; Jones, L. E. (eds.) Advances in Fusion and Processing of Glass II. Proc. 5th Int. Symp. Advances and Processing of Glass, Toronto 1997. Westerville, OH: Am. Ceram. Soc., 1998. p. 187–202. (Ceram. Trans. Vol. 82.)
[24] Mattson, S. M.: Recent developments in in-vitro testing of fiber biopersistence. The effect of forming. In: Proc. XVIII International Congress on Glass. San Francisco, CA 1998. C5 p. 23–28. (Available on CD-ROM from The American Ceramic Society, Westerville, OH.)

0200P003

Address of the author:

R. M. Potter
Owens Corning
Science and Technology Center
2790 Columbus Road, Route 16
Granville, OH 43023.1200
USA